



EUROPEAN ORGANIZATION FOR NUCLEAR RESEARCH

CERN/EP 87-108  
19 June 1987

INCLUSIVE PRODUCTION OF  $\rho^0$  AND  $f_2$  MESONS

IN  $\pi$ -p INTERACTIONS AT 360 GeV/c

LEBC-EHS Collaboration

Antwerp/Brussels<sup>1</sup>-Berlin<sup>2</sup>-Bombay<sup>3</sup>-CERN<sup>4</sup>-Genova<sup>5</sup>-Madrid<sup>6</sup>-Mons<sup>7</sup>-  
Moscow<sup>8</sup>-Padova<sup>9</sup>-Paris<sup>10</sup>-Roma<sup>11</sup>-Serpukhov<sup>12</sup>-Stockholm<sup>13</sup>-Trieste<sup>14</sup>-Vienna<sup>15</sup>

J.L. Bailly<sup>7</sup>, S. Banerjee<sup>3</sup>, E. Castelli<sup>14</sup>, P. Checchia<sup>9</sup>, P.V. Chliapnikov<sup>12</sup>,  
N. Colino<sup>6</sup>, R. Contri<sup>5</sup>, A. De Angelis<sup>9</sup>, A. De Roech<sup>1</sup>, N. De Seriiis<sup>11</sup>,  
J. Duboc<sup>10</sup>, P.F. Ermolov<sup>8</sup>, S. Falciano<sup>11</sup>, Y.V. Fisjak<sup>12</sup>, F. Fontanelli<sup>5</sup>,  
U. Gasparini<sup>9</sup>, S. Gentile<sup>11</sup>, Y.A. Golubkov<sup>8</sup>, J.J. Hernandez<sup>6</sup>, S.O. Holmgren<sup>13</sup>,  
J. Hrubec<sup>15</sup>, M. Iori<sup>11</sup>, M.I. Josa<sup>6</sup>, K.E. Johansson<sup>13</sup>, E.P. Kistenev<sup>12</sup>,  
D. Knauss<sup>2</sup>, V.V. Kniازه<sup>12</sup>, E.A. Kozlowski<sup>12</sup>, V.M. Kubik<sup>12</sup>, M. Mazzucato<sup>9</sup>,  
R. Monge<sup>5</sup>, L. Montanet<sup>4</sup>, H. Nowak<sup>2</sup>, H.K. Nguyen<sup>9</sup>, V.M. Perevoztchikov<sup>12</sup>,  
P. Pilette<sup>7</sup>, A. Poppleton<sup>6</sup>, P. Poropat<sup>14</sup>, R. Raghavan<sup>3</sup>, H. Rohringer<sup>15</sup>,  
J.M. Salicio<sup>6</sup>, M. Sessa<sup>14</sup>, E.K. Shabalina<sup>8</sup>, N.A. Sotnikova<sup>8</sup>, S. Squarcia<sup>5</sup>,  
V.A. Stopchenko<sup>12</sup>, U. Trevisan<sup>5</sup>, C. Troncon<sup>14</sup>, F. Verbeure<sup>1</sup>, J.V. Yarba<sup>8</sup>  
and G. Zumerle<sup>9</sup>

- 1 Inter-University Institute for High Energies Brussels and Dept. of Physics, Universitaire Instelling Antwerpen, Wilrijk, Belgium
- 2 Institut für Hochenergiephysik der AdW der DDR, Berlin-Zeuthen, GDR
- 3 Tata Institute for Fundamental Research, Bombay, India
- 4 CERN, European Organization for Nuclear Research, Geneva, Switzerland
- 5 INFN and University of Genoa, Italy
- 6 CIEMAT-JEN, Madrid, Spain
- 7 University of Mons, Mons, Belgium
- 8 Moscow State University, Moscow, USSR
- 9 INFN and University of Padua, Italy
- 10 LPNHE, University of Paris VI, France
- 11 Dept. of Physics, University of Rome, Italy
- 12 Institute for High Energy Physics, Serpukhov, USSR
- 13 Dept. of Physics, University of Stockholm, Sweden
- 14 Institute for Physics, University of Trieste, Italy
- 15 IHEP, Vienna, Austria

Submitted to Zeitschrift für Physik C

## Abstract

We report on a study of  $\rho^0$  and  $f_2$  inclusive production in  $\pi^-$ -p interactions at 360 GeV/c, using the LEBC-EHS set-up at CERN and reconstructing about 165,000 events. The  $\rho^0$ ,  $f_2$  and  $\rho_3^0$  cross sections are determined for  $x_F > 0$ ,  $x_F > 0.4$  and  $x_F > 0.6$  respectively and the  $\rho^0$  and  $f_2$  Feynman-x distributions and transverse momentum distributions are presented.

## 1. INTRODUCTION

The study of resonance production in high-energy interactions is primarily motivated by our understanding that resonances, being a more direct product of the collisions, reflect more closely the dynamical mechanisms involved than the final particles, the majority of which originates from resonance decay.

Previous results indicate that at high energies vector-meson production is as important as the production of pseudoscalar mesons. This is in qualitative agreement with spin statistics [1]-[2], which predicts that most observed particles are decay products of vector meson resonances. Detailed quark-parton models give quantitative predictions on the behaviour of vector meson production [3]-[4].

The study of resonances in inclusive reactions is however a difficult task because of poor particle identification in the majority of the experiments, large combinatorial backgrounds especially at high energies, limited acceptance or momentum resolution in many experiments and very often insufficient statistics. Therefore, even data on the abundantly produced  $\rho^0(770)$  are quite scarce at high energies.

The purpose of this paper is to present new data on the forward production of  $\rho^0(770)$ ,  $f_2(1270)$  and  $\rho_3^0(1670)$  in the inclusive reactions

$$\pi^- p \rightarrow \rho^0(770) + X \quad (1)$$

$$\pi^- p \rightarrow f_2^0(1270) + X \quad (2)$$

$$\pi^- p \rightarrow \rho_3^0(1670) + X \quad (3)$$

at 360 GeV/c from an experiment with minimum bias trigger and high statistics. Our results on reaction (1) differ significantly from the ones of another experiment at 360 GeV/c [5], the highest momentum so far reached for pion induced reactions.

The paper is organised as follows. The experimental set-up, the data handling and the fitting procedures are described in Sections 2 to 4. In Section 5 results are given on the inclusive cross sections, invariant and non-invariant Feynman-x distributions and on the  $p_T^2$  distributions for the  $\rho^0$  and  $f_2$ .

## 2. THE EXPERIMENTAL SET-UP

The NA27 experiment was carried out with the European Hybrid Spectrometer (EHS) [6], exposed to a negative pion beam of 360 GeV/c momentum and aimed at a detailed study of hadronic production and properties of charmed particles. The EHS set-up and performance of the detectors are described in [7]. Its main ingredients are the high resolution bubble chamber, serving both as a target and as a vertex detector, and the spectrometer for

momentum analysis and particle identification. Its geometrical acceptance was defined mainly by the gap of the magnet in the first level arm. For charged particles it is  $\pm 200$  mrad vertically (in the bending plane) and  $\pm 90$  mrad horizontally; at our energy this corresponds to 100% coverage of the forward hemisphere in the c.m. system. One million bubble chamber pictures were taken with the pion beam, corresponding to a total sensitivity of  $\approx 17$  events/ $\mu\text{b}$ .

The data taking was triggered by a simple interaction trigger [8] demanding three or more hits in each of the two trigger wire chambers. It was supplemented with a specially designed fiducial volume trigger to reject interactions outside the bubble chamber sensitive volume. The triggered fraction of the total inelastic cross section was found to be  $(80.3 \pm 4.5)\%$ , where the losses are mainly at the low multiplicities. These losses are uncontrollable for the two-prong events and the latter were excluded from further analysis. For the higher multiplicities the losses were accounted for by proper normalization to the known topological cross sections. Details of the weighting procedure can be found in [9].

### 3. DATA HANDLING

The present analysis is based upon about two thirds of the  $\pi^-$  triggers defined in the previous section. The event reconstruction was preceded by film scanning. The scanning information was used to select only those triggers corresponding to a primary interaction within the effective volume of the bubble chamber, giving a clean sample of 165,000 interactions of primary  $\pi^-$  mesons in hydrogen, corresponding to a sensitivity of  $\approx 8$  events/ $\mu\text{b}$ .

During scanning only the primary multiplicity and the coordinates of the primary vertex were recorded since the spectrometer data alone are sufficient to achieve a high efficiency of track reconstruction and no extra measurement of the bubble chamber pictures was needed to match the tracks with the primary interaction.

The events were processed with a multi-step track-reconstruction program. First track-segments were reconstructed in the spectrometer. For those tracks having matched segments in the first and second level arm the momentum estimates were computed using the bending angle in the second magnet. All track candidates were backtraced to the interaction point, thus giving an estimate for the momenta of the tracks reconstructed only in the first level arm. This procedure was iterated, improving the coordinates of the primary vertex and keeping the track candidates missing the vertex in the non-bending plane as hanging ones. In a last stage the final values for the momenta and angles were computed using the reconstructed vertex position and all hits in the wire chambers (starting from the zero-level arm, i.e. before the first magnet) associated with a given candidate. Track candidates left aside as hanging were then paired in an attempt to reconstruct neutral

strange particle decays in the spectrometer.

Details of the data-handling, including a detailed discussion of the acceptance computation, will be published in a separate paper [9]. Nevertheless it is worthwhile to indicate here some results which are relevant to the purposes of the present study.

The efficiency of the track reconstruction was obtained by measuring a non-biased sample of about 3,000 events and processing these events through two independent reconstruction chains – one described above and another one used for charmed events (the standard NA27 geometry makes full use of the bubble chamber measurements). The efficiency of the latter is well known and described elsewhere [7]. The single particle efficiency for track reconstruction increases from  $\approx 70\%$  at  $x_F=0$  to  $90\%$  at  $x_F=1$  and was parametrized using a smooth function depending on the kinematical track-parameters (charge, momentum and angles). Using a parametrization of this type we were able to avoid systematic uncertainties in the further acceptance computations for two-body meson decays, independently of the resonance decay characteristics, as was checked by Monte Carlo simulations.

In what follows each two-particle combination was given a weight equal to the product of the efficiencies derived from the single particle acceptance curves. No identification information was used in this study.

#### 4. DATA ANALYSIS

The invariant mass spectra of  $\pi^+\pi^-$  were formed. All primary tracks were assumed to be pions. The mass spectrum for  $x_F > 0$  and  $x_F > 0.6$  are shown in Fig.1. The  $\rho^0$  signal is clearly seen in all  $x_F$ -intervals, while the  $f_2$  and  $\rho_3^0$  can only be detected for  $x_F > 0.4$  and  $x_F > 0.6$  respectively. The signal to background ratio for all resonances improves significantly with increasing  $x_F$ .

The resonance cross sections were determined by fits of the weighted  $\pi^+\pi^-$  mass distributions in a given  $x_F$  or  $p_T^2$  interval to the expression

$$d\sigma/dM = BG(p^*)(1 + \alpha_1 BW_1 + \alpha_2 BW_2 + \alpha_3 BW_3) \quad (4)$$

where  $p^*$  is computed with the well known  $\lambda$  function:

$$p^* = (1/2M)\sqrt{\lambda(M^2; m_\pi^2, m_\pi^2)}$$

$BW_i(M)$  are relativistic P-, D- and F-wave Breit-Wigner functions;  $\alpha_1, \alpha_2, \alpha_3$  are fitted parameters (in absence of  $f_2$  and  $\rho_3^0$  contributions the values of  $\alpha_2$  and  $\alpha_3$  were fixed at zero).

After testing of different background (BG) parametrizations on a sample of Lund generated events [10], the following choice was found to be optimal:

$$BG(p^*) = (p^*/M)^\beta \cdot \exp(-\gamma p^* - \delta p^{*2})$$

where  $\beta$ ,  $\gamma$  and  $\delta$  are again fitted parameters.

The total width of each resonance was assumed to be the sum of the natural width of the resonance and the width of the experimental resolution function. The central masses and natural widths of the resonances were fixed at the values given in the Particle Data Group tables [11].

## 5. RESULTS

The forward ( $x_F > 0$ )  $\rho^0$  cross section in reaction (1) is equal to  $(6.35 \pm 0.24 \pm 0.40)$  mb, where the first error is statistical and the second represents our estimate of the systematical uncertainty<sup>1</sup>. In Fig. 2 it is compared with the forward and total inclusive  $\rho^0$  cross sections in other  $\pi^\pm p$  experiments. The forward  $\rho^0$  cross sections in  $\pi^- p$  interactions at 100, 200 and 360 GeV/c [5] measured in the Fermilab hybrid spectrometer<sup>2</sup> appear to be inconsistent with the trend of other data and this inconsistency is larger at 360 GeV/c than at 100 GeV/c. In particular, their cross section at 360 GeV/c is almost twice lower than in our experiment, presumably due to a significant loss of resolution in their downstream spectrometer. On the other hand, the 30-inch hydrogen bubble chamber provides accurate measurements for the low-momentum tracks [5] and one can expect that the backward ( $x_F < 0$ )  $\rho^0$  cross section  $(5.14 \pm 0.25)$  mb at 360 GeV/c is measured correctly. Adding this value and the forward  $\rho^0$  cross section measured in our experiment, we obtain for the total  $\rho^0$  inclusive cross section at 360 GeV/c the value of  $(11.5 \pm 0.4 \pm 0.4)$  mb, which is in good agreement with the trend of the lower energy data [5, 12–20] in Fig. 2. This value is also consistent with the preliminary result of  $(10.5 \pm 2.0)$  mb for the total inclusive  $\rho^0$  cross section in 360 GeV/c pp interactions [21]. A fit of the s-dependence of the total  $\rho^0$  cross section in  $\pi^\pm$  interactions to the form  $\sigma_{tot}^{\pi^\pm p}(\rho^0) = a + b \cdot \ln s$ , obtained using this value of the cross section at 360 GeV/c, but not the Fermilab points, gives  $b = (2.0 \pm 0.2)$  mb. A similar fit to the s-dependence of the forward  $\rho^0$  cross section in  $\pi^\pm p$  interactions, again without the Fermilab points, yields  $b = (0.9 \pm 0.1)$  mb. The results of these fits are shown in Fig. 2 by the straight lines.

---

<sup>1</sup> Subsequently we give the statistical errors only.

<sup>2</sup> The forward and backward  $\rho^0$  cross sections for the Fermilab data have been obtained by us, using Fig. 8 of ref. [5] and checking the results obtained with table 5 of ref. [5], assuming a uniform  $d\sigma(\rho^0)/dy^*$  distribution in the interval  $-1 < y^* < 1$ .

The  $\rho^0$ ,  $f_2^0$  and  $\rho_3^0$  cross sections in  $\pi^-p$  interactions at 360 GeV/c for the regions of large  $x_F$  are presented in Table 1. We see that the  $f_2^0/\rho^0$  ratio is as large as  $0.45\pm 0.05$  ( $0.50\pm 0.06$ ) for  $x_F > 0.4$  ( $x_F > 0.6$ ) and that  $\rho_3^0/f_2^0 \approx 0.9\pm 0.2$  for  $x_F > 0.6$ .

The  $d\sigma/dx$  and Lorentz-invariant  $F(x_F)=2\pi \int (E^*d^3\sigma/d^3p)dp_T^2$  distributions for the  $\rho^0$  and  $f_2$  are presented in Fig. 3. The  $\rho^0$ -meson  $F(x_F)$ -distribution (Fig. 3b) is practically flat in the region  $0 < x_F < 0.8$ , while for  $x_F > 0.8$  one observes a prominent peak with maximum at  $x_F \approx 0.87$ , which is also evident in the non-invariant distribution (Fig. 3a). A similarly pronounced peak is also present in the  $F(x_F)$  distribution for the  $f_2^0$  meson (Fig. 3b). In Fig. 3b we compare the  $F(x_F)$  distribution of the  $\rho^0$  at 360 GeV/c with the one at 16 GeV/c [12]. The two distributions scale within errors, although our points are slightly lower than the data at 16 GeV/c.

The position of the peaks in the  $F(x_F)$ -spectra of the  $\rho^0$  and  $f_2^0$  suggests their interpretation as diffractive-like components for the  $\rho^0$  and  $f_2^0$  production in reactions (1) and (2). A rough estimate of this component for the  $\rho^0$  can be obtained by comparing the  $d\sigma/dx$  spectrum with the predictions of the Lund fragmentation model [22], which has no diffractive dissociation contribution. The Lund Monte Carlo<sup>1</sup> yields 10.3 mb for the total and 6.3 mb for the forward  $\rho^0$  production cross section in reaction (1), in reasonable agreement with our results. In Fig. 3a we show the model prediction for the  $d\sigma/dx$  spectrum, normalized to the data in the interval  $0 < x_F < 0.5$ . It describes the shape of the distribution reasonably well, apart from the region of large  $x_F$  where the diffractive contribution is most important. The difference between the experimental and the Lund  $d\sigma/dx$  spectra thus provides an estimate of 0.6 mb for the diffractive component of the  $\rho^0$  production cross section in reaction (1), which amounts to  $\approx 5\%$  of the corresponding total  $\rho^0$  cross section. It is of interest to note that the relative contribution of the diffractive cross section to the total inclusive cross section is about the same ( $\approx 5\%$ ) for many different processes, such as  $K_{dif}^+ \rightarrow K^*(890)X$ ,  $K^*(1430)X$  [23],  $K_{dif}^+ \rightarrow K_S^0X, \Lambda X, \bar{\Lambda}X$  [24],  $K_{dif}^+ \rightarrow \phi X$  [25],  $p_{dif} \rightarrow K_S^0X, \Lambda X, \bar{\Lambda}X$  [26], etc.

The  $\rho^0$  invariant  $p_T^2$  distributions  $F(p_T^2) = 2\pi \int (E^*d^3\sigma/d^3p)dp_L$ , integrated over the intervals  $0 \leq x_F \leq 0.5$  and  $x_F \geq 0.5$  are presented in Fig. 3a and 3b respectively. The former is described by a single exponential  $A \cdot \exp(-bp_T^2)$  with slope parameter  $b = (3.05 \pm 0.16) (\text{GeV}/c)^{-2}$ . The latter can only be described by a sum of two exponentials with slope values of  $(10.5 \pm 1.7) (\text{GeV}/c)^{-2}$  and  $(2.5 \pm 0.2) (\text{GeV}/c)^{-2}$  respectively. The presence of a steep component in the  $\rho^0$  invariant  $p_T^2$  distribution for  $x_F > 0.5$  can be explained as decay

---

<sup>1</sup> We used the standard version of the Lund model of ref. [22], modified to include contributions from tensor (T) mesons in the proportion T:V=0.3:0.7 to the vector (V) mesons at the generation stage.

products of diffractively produced higher mass states. The  $f_2^0$  invariant  $p_T^2$ -distribution integrated over the  $x_F > 0.4$  interval (not shown) is consistent within errors with a single exponential with slope equal to  $(4.2 \pm 1.1)(\text{GeV}/c)^{-2}$ .

## 6. SUMMARY

A high statistics study is made of  $\rho^0$ ,  $f_2^0$  and  $\rho_3^0$  production in  $\pi^-p$  interactions at 360 GeV/c, using the spectrometer information of the European Hybrid Spectrometer. The methods used are briefly explained. The inclusive production cross sections for  $\rho^0$ ,  $f_2^0$  and  $\rho_3^0$  amount to  $(6.35 \pm 0.24)$  mb for  $\rho^0$  at  $x_F > 0.$ ,  $(0.74 \pm 0.07)$  mb for  $f_2^0$  at  $x_F > 0.4$  and  $(0.42 \pm 0.09)$  mb for  $\rho_3^0$  at  $x_F > 0.6$ . Using an estimate for the backward  $\rho^0$  cross section from another independent experiment [5], we derive a total  $\rho^0$  cross section of  $(11.5 \pm 0.4)$  mb, consistent with a  $\ln s$  increase but considerably larger than the previously published value [5]. From the Feynman-x spectra, both invariant and non-invariant, as well as from the  $p_T^2$  distributions, we deduce that an important fraction of the very forward produced  $\rho^0$  can be ascribed to decay products of diffractively produced states. The fraction of these is estimated at  $\approx 5\%$ , consistent with observations in  $K^+p$  interactions [23–26].

### *Acknowledgements*

We wish to thank all the people in the various laboratories who have contributed to the construction, operation and analysis of this experiment, including the CERN staff operating the SPS beam. We are particularly grateful to F. Bruyant for his tremendous contributions to the reconstruction programs and to V.A. Uvarov for discussions and help with the fit programs.



**Table 1.** The  $\rho^0(770)$ ,  $f_2^0(1270)$  and  $\rho_3^0(1670)$  cross sections in mbarn, corrected for unobserved decay modes, in reactions (1)–(3) for the regions of large  $x_F$ . Systematic errors are not included; they are about twice larger than the statistical errors.

Reaction	Cross section (in mbarn)	
	$x_F > 0.4$	$x_F > 0.6$
$\pi^- p \rightarrow \rho^0(770)X$	$1.65 \pm 0.05$	$0.94 \pm 0.04$
$\pi^- p \rightarrow f_2^0(1270)X$	$0.74 \pm 0.07$	$0.47 \pm 0.05$
$\pi^- p \rightarrow \rho_3^0(1670)X$	—	$0.42 \pm 0.09$

## REFERENCES

- [1] V.V. Anisovich and V.M. Shekhter, Nucl. Phys. **B55**, 45 (1973)
- [2] V.M. Shekhter and L.M. Shcheglova, Sov. J. Nucl. Phys. **27**, 567 (1978)
- [3] S. Nandi, V. Rittenberg and H.R.Schnider, Phys. Rev. **D17**, 1336 (1978)
- [4] K.V. Vasavada, Phys. Rev. **D20**, 2304 (1979)
- [5] P.D. Higgins et al., Phys. Rev. **D19**, 65 (1979)
- [6] M. Aguilar-Benitez et al., Nucl. Instr. & Methods **205**, 79 (1983)
- [7] M. Aguilar-Benitez et al., Z. Physik C, Particles and Fields, **31**, (1986), 491.
- [8] R. Bizzari et al., "The NA27 Trigger", Preprint USIP Report 85-10.
- [9] Y. Fisjak et al., *Minimum bias events from EHS*, in preparation
- [10] B. Andersson et al., Nucl. Phys. **B178** (1981) 242; Phys. Reports **C97** (1983) 31
- [11] Particle Data Group: M. Aguilar-Benitez et al., Phys. Lett. **170B**, 1 (1986)
- [12] J. Bartke et al., Nucl. Phys. **B 107**, 93 (1976)
- [13] M. Deutschman et al., Nucl. Phys. **B103** (1976) 426.
- [14] K. Böckmann et al., Nucl. Phys. **B 140**, 245 (1978)
- [15] H.A. Gordon et al., Phys. Rev. Lett. **34** (1975) 284
- [16] I.V. Ajinenko et al., Preprint IHEP 79-111
- [17] J. Bran et al., Nucl. Phys. **B 99**, 232 (1975)
- [18] M. Schouten et al., Z. Physik C, Particles and Fields, **9**, (1981), 93.
- [19] Amaglobelli et al., Yad. Fiz. **37** (1983) 624
- [20] N.S. Angelov et al., Yad. Fiz. **33** (1981) 1539
- [21] Private communication from the NA23 collaboration
- [22] B. Andersson et al., Nucl. Phys. **B 178**, 242 (1981) ; Phys. Rep. **C97**, (1983) 31
- [23] P.V. Chliapnikov et al., Z. Physik C, Particles and Fields, **12**, (1982), 113.
- [24] I.V. Ajinenko et al., Z. Physik C, Particles and Fields, **23**, (1984), 307.
- [25] I.V. Ajinenko et al., Yad. Fiz. **39** (1984) 1448
- [26] M. Asai et al., Z. Physik C, Particles and Fields, **27**, (1985), 11.

## FIGURE CAPTIONS

- Fig. 1 a) Invariant  $\pi^+\pi^-$  mass spectrum for  $x_F > 0$ . (a) and  $x_F > 0.6$  (b). The curves describe the fit to the expression (4) (see text).
- Fig. 2 The total inclusive  $\rho^0$  and the forward ( $x_F > 0$ ) cross section in  $\pi^\pm p$  reactions as a function of c.m. energy squared  $s$ . The straight lines are fits to the expression  $a + b \ln s$ . The data are from refs. [5, 12-20].
- Fig. 3 Non-invariant (a) and invariant (b) Feynman-x distributions for  $\rho^0$  (crosses) and  $f_2^0$  (stars). The curve in (a) is the prediction of the Lund model, normalized to the data in the  $0 < x_F < 0.5$  interval. The  $\pi^- p$  data at 16 GeV/c (open circles in Fig. 3b) are from ref. [12].
- Fig. 4 The  $F(p_T^2)$  distributions for  $\rho^0$  in the intervals  $0 \leq x_F \leq 0.5$  (a) and  $x_F \geq 0.5$  (b).

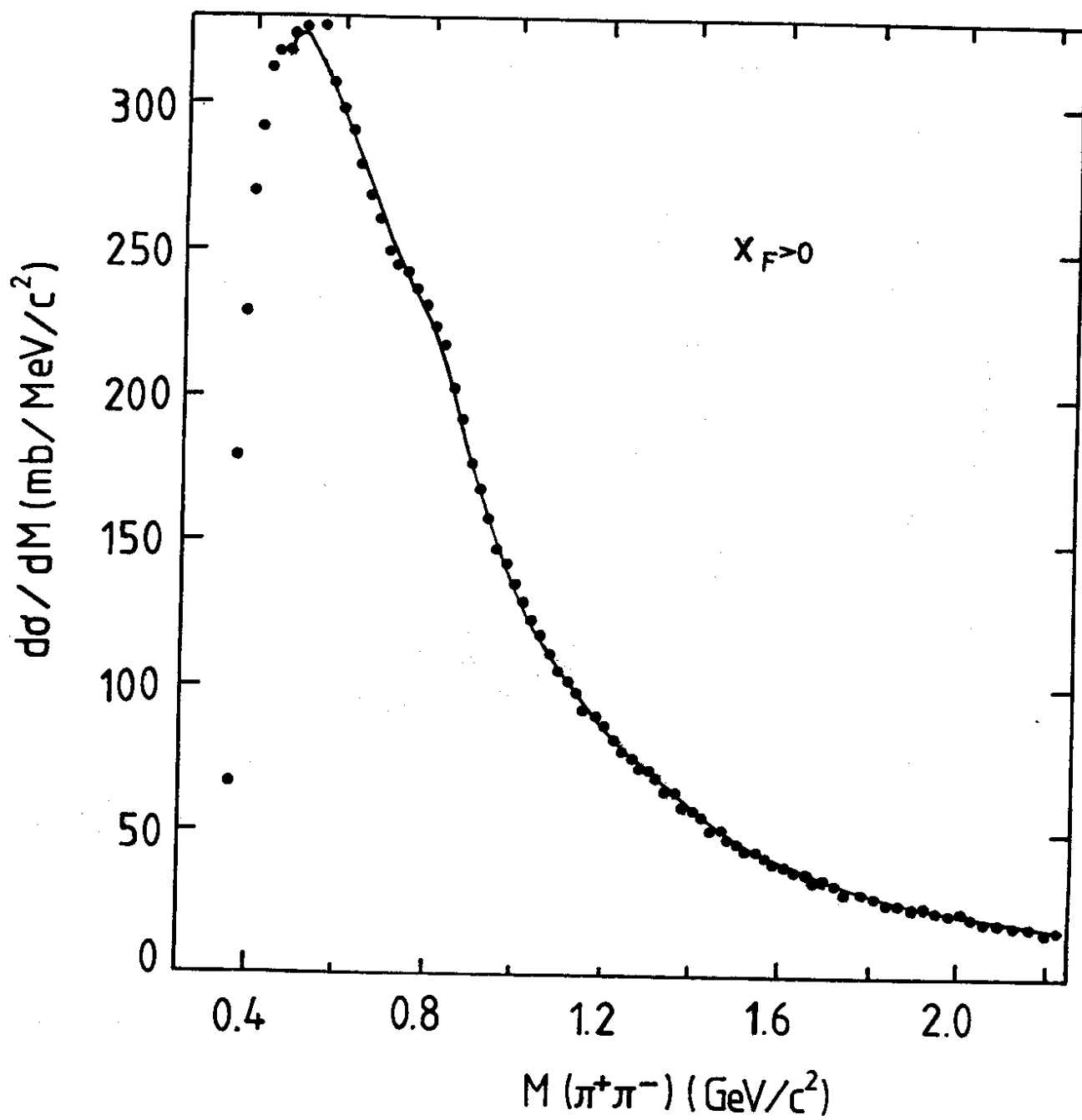


Fig. 1a

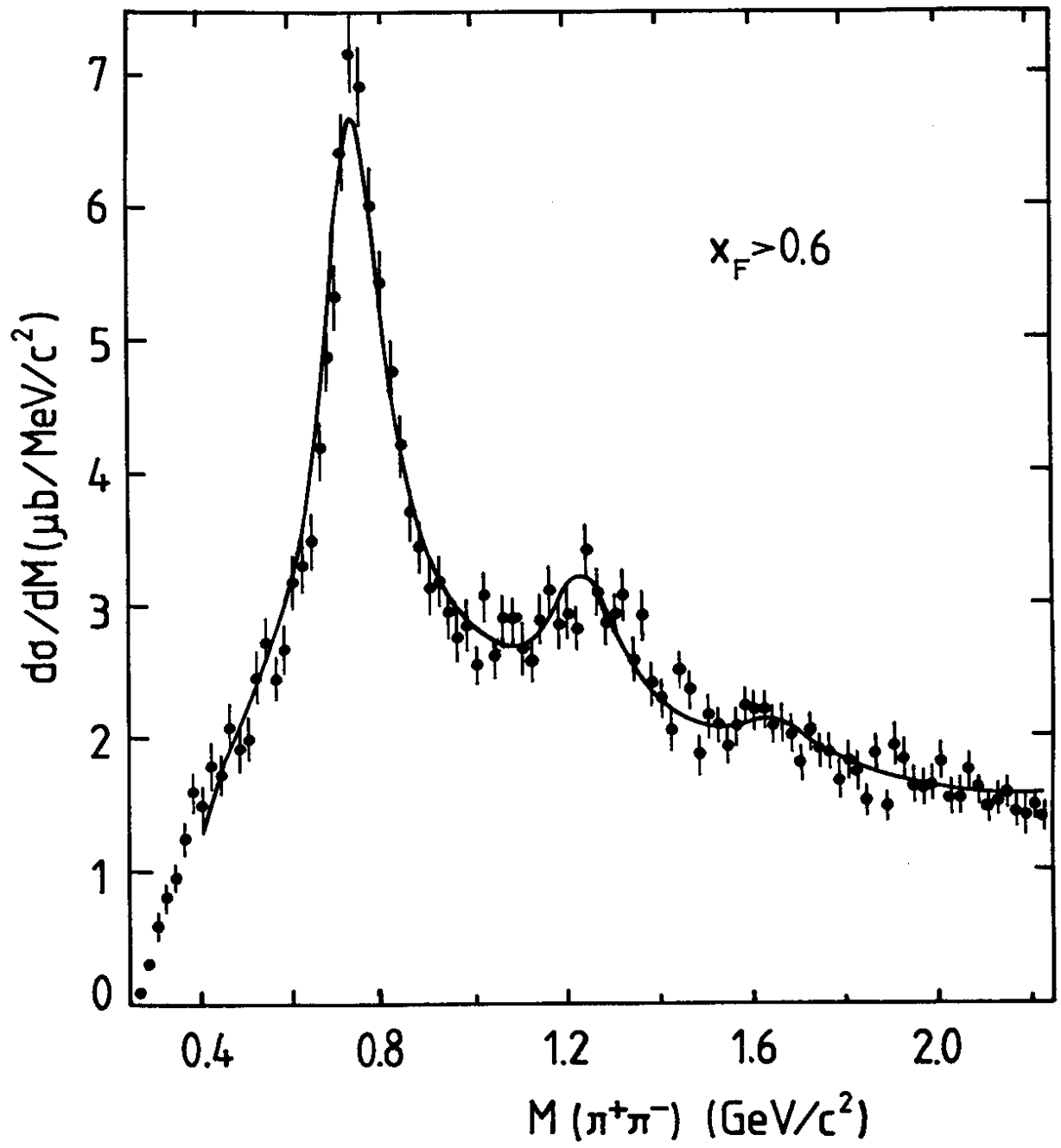


Fig. 1b

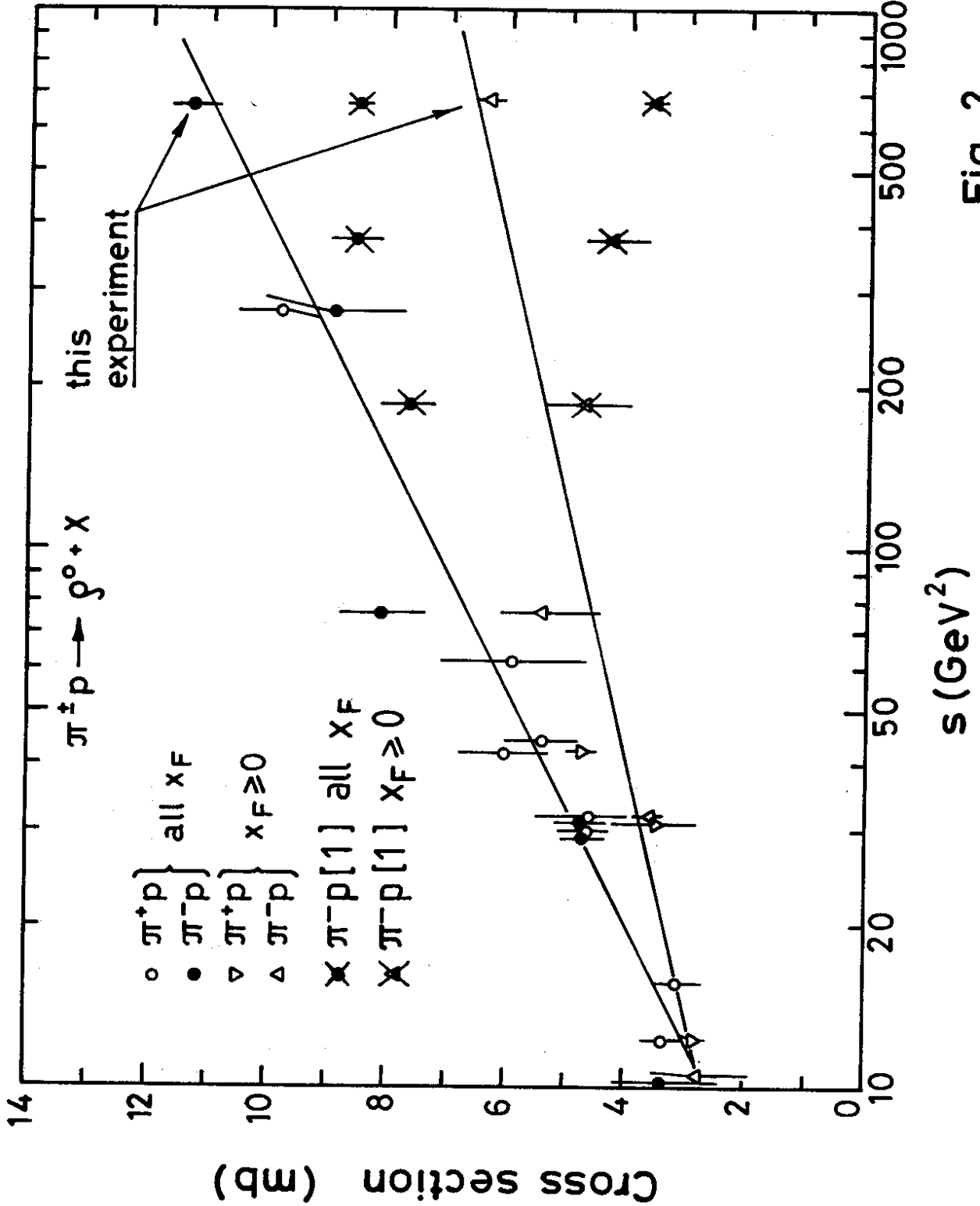


Fig. 2

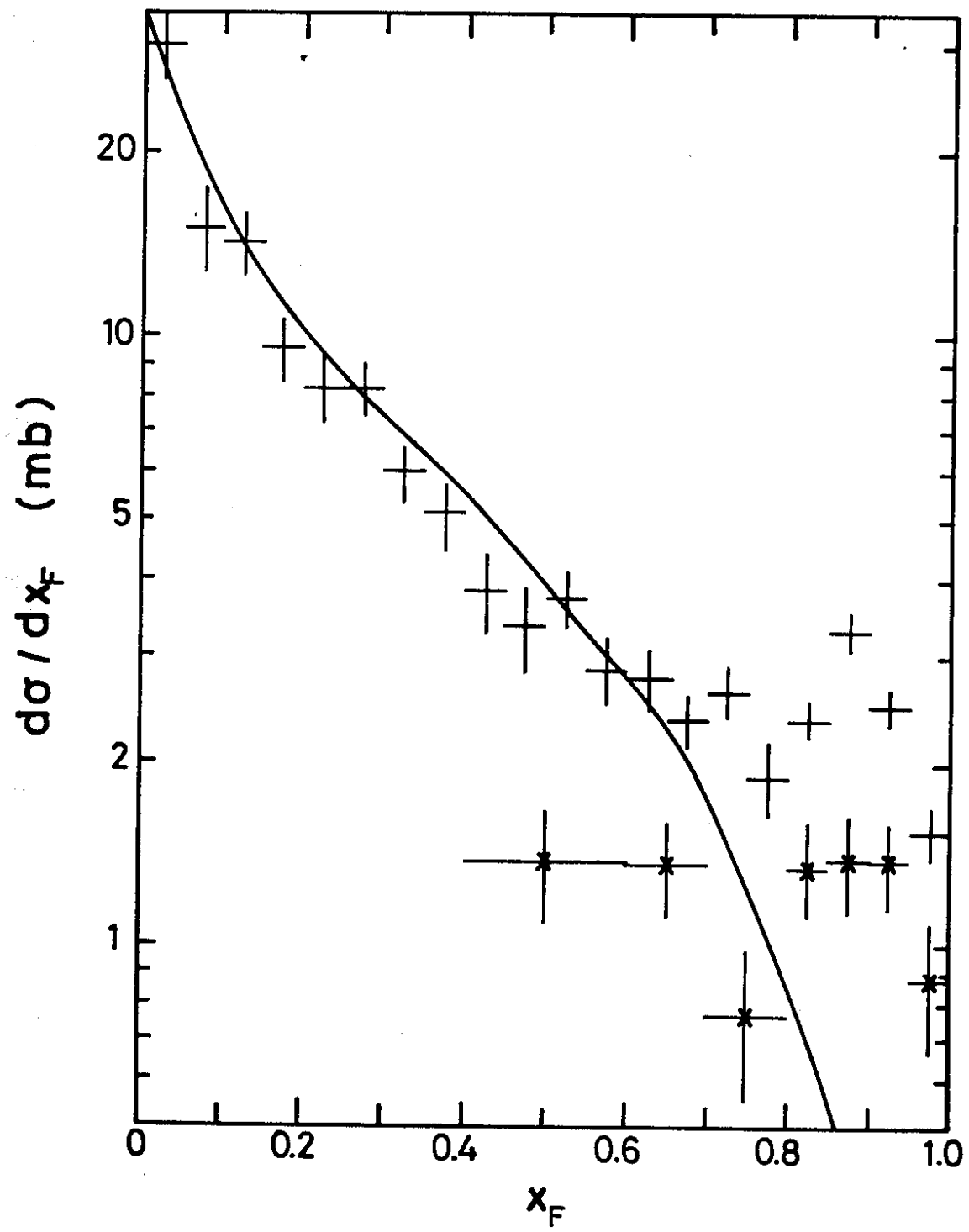


Fig. 3a

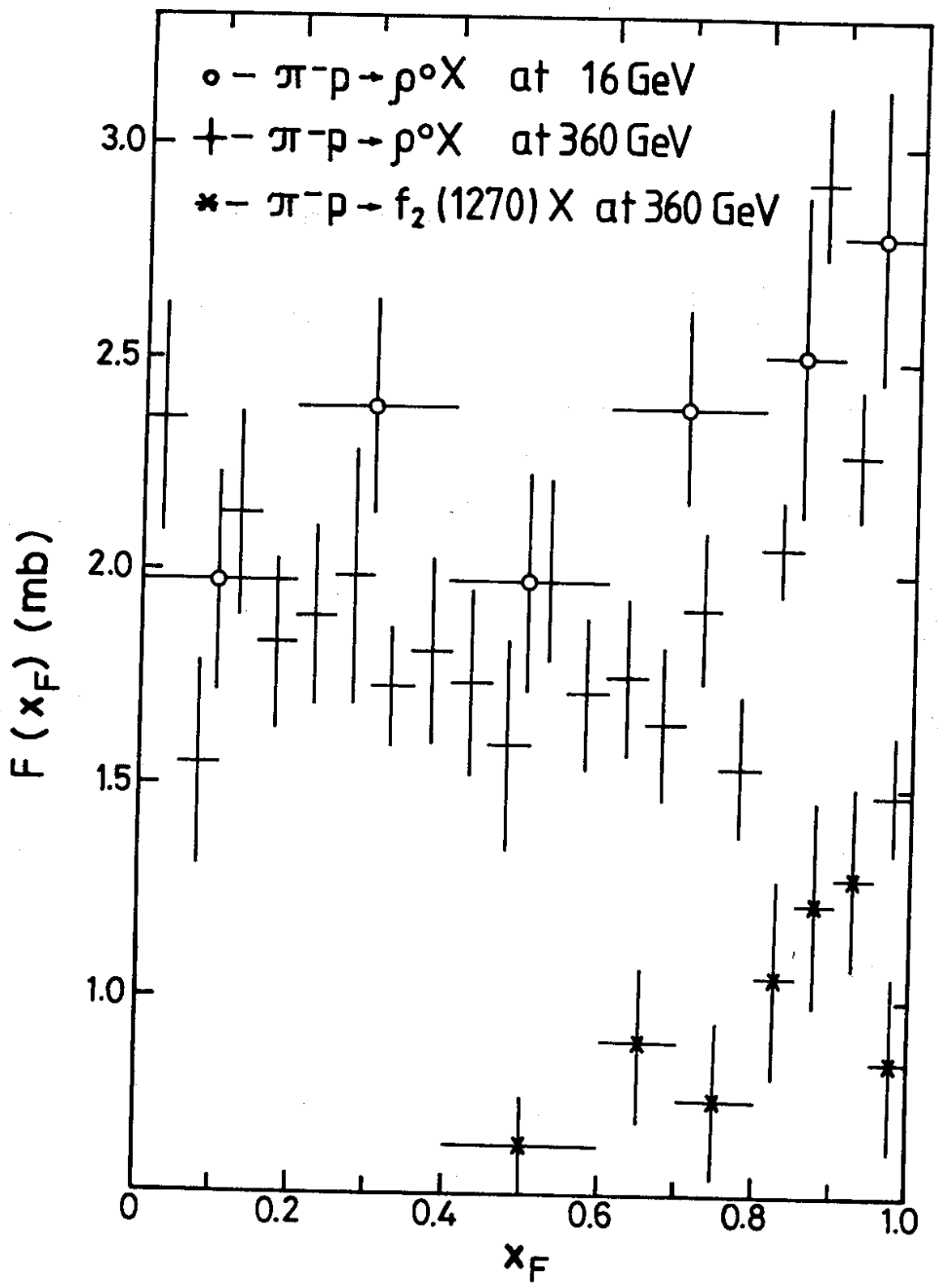


Fig. 3b

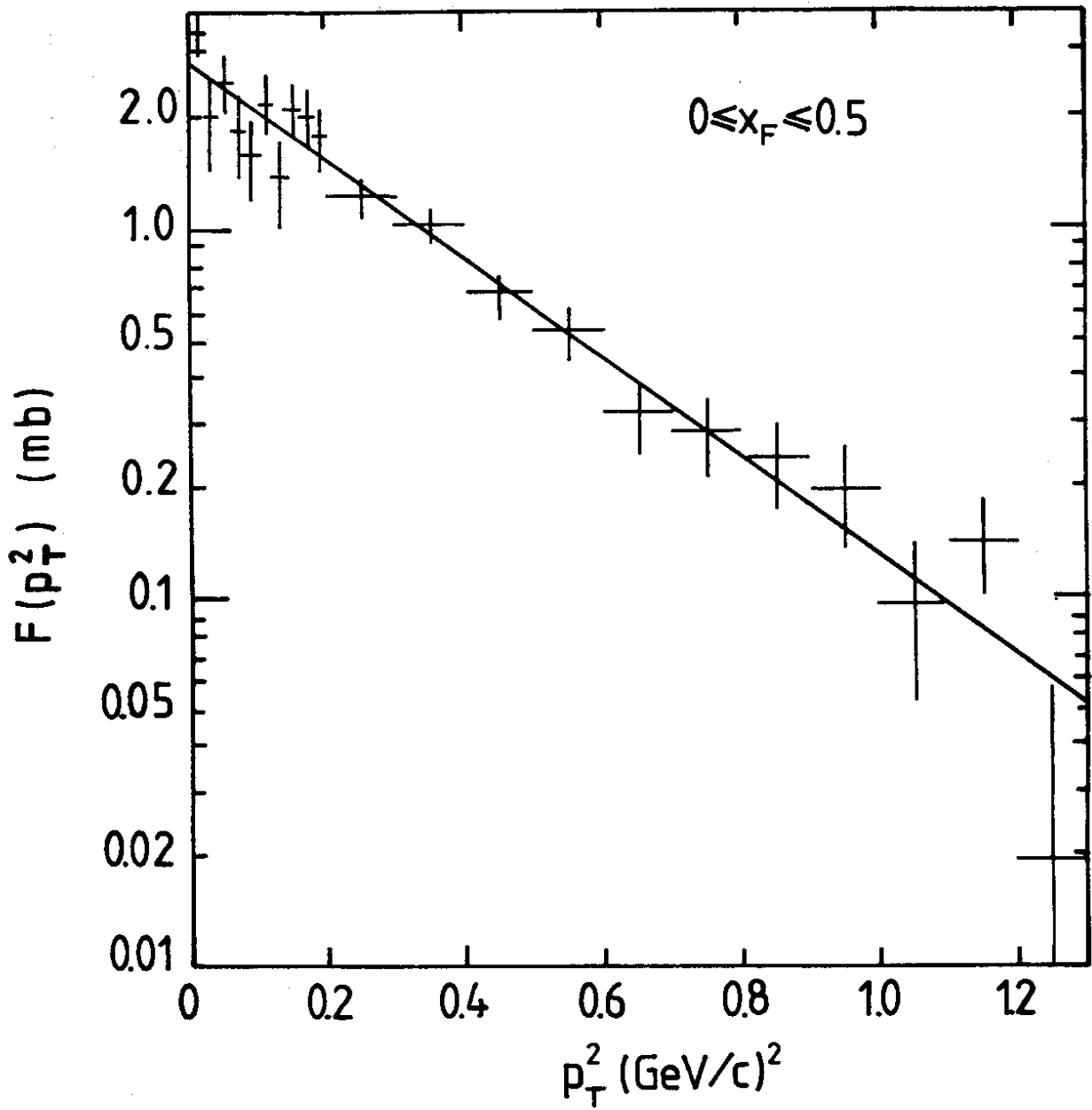


Fig.4a



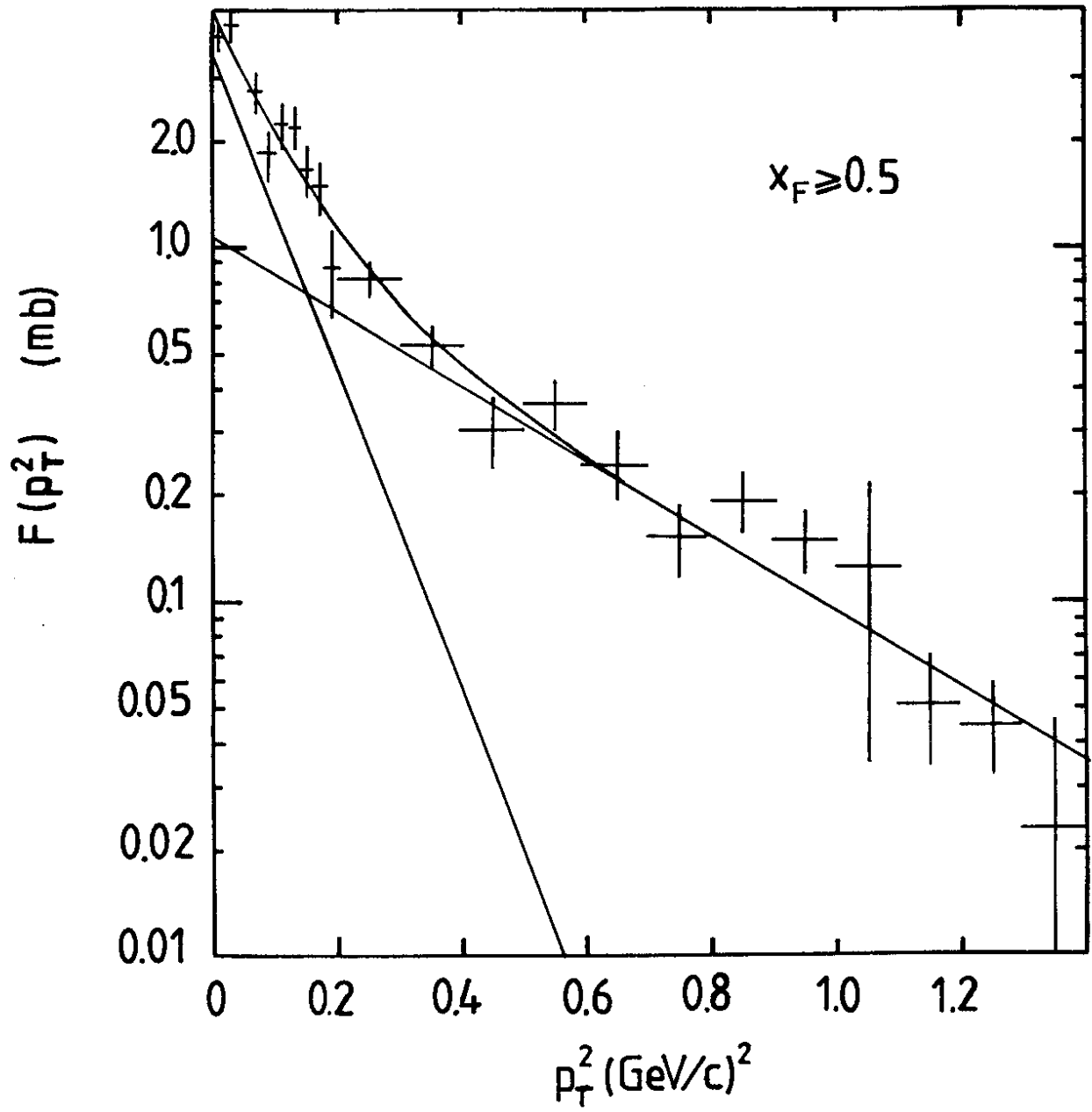


Fig. 4b